Annals of Nuclear Medicine Vol. 18, No. 3, 263–270, 2004

Renal accumulation and excretion of radioiodinated 3-iodo-α-methyl-L-tyrosine

Naoto SHIKANO,* Keiichi KAWAI,** Syuichi NAKAJIMA,** Ryuichi NISHII,*** Leo Garcia FLORES II,*** Akiko KUBODERA,**** Nobuo KUBOTA,* Nobuyoshi ISHIKAWA* and Hideo SAJI*****

*Department of Radiological Sciences, Ibaraki Prefectural University of Health Sciences
**School of Health Sciences, Faculty of Medicine, Kanazawa University
***Department of Radiology, Miyazaki Medical College
****Faculty of Pharmaceutical Sciences, Science University of Tokyo
*****Graduate School of Pharmaceutical Sciences, Kyoto University

Objective: We investigated mechanisms of renal accumulation of radioiodinated 3-iodo-α-methyl-L-tyrosine (IMT), which has been used clinically for tumor imaging and as an amino acid transport marker in studies of brain and pancreas function. ***Methods:*** In this study, we used ^{125}I- or ^{123}I-labeled IMT ([^{125}I]IMT or [^{123}I]IMT) as the transport marker. Partition coefficients of [^{125}I]IMT were determined for hypothetic urine at pH ranging from 5 to 8. The examination of uptake and inhibition of [^{125}I]IMT was performed using normal human renal proximal tubule epithelial cells (RPTEC), which are characteristic of the proximal convoluted tubule. The plasma protein binding ratio of [^{125}I]IMT was determined using rats. In the *in vivo* experiments using mice, we examined biodistribution and excretion inhibition, and performed whole body autoradiography. Also, renal SPECT using [^{123}I]IMT was performed using a normal canine. ***Results:*** Very low lipophilicity of [^{125}I]IMT in hypothetic urine suggests that a carrier-mediated pathway contributes to its marked kidney accumulation. [^{125}I]IMT uptake into RPTEC was significantly inhibited by 2-aminobicyclo[2,2,1]heptane-2-carboxylic acid (BCH) in a sodium-dependent manner, suggesting reabsorption mainly via system B^0 in apical membrane of proximal tubule. Plasma protein binding ratio of IMT was 45.4 ± 5.6%. At 6 hr after administration of IMT to mice, excretion via urinary tract was 77.51% of injected dose, and excretion into feces was 0.25%. Furosemide, ethacrynic acid and probenecid inhibited tubular secretion of [^{125}I]IMT in mice. We obtained very clear autoradiographs of mouse renal cortex and a canine renal SPECT image (S2-like region). ***Conclusions:*** We believe that [^{123}I]IMT is useful for kidney imaging. In future studies, we plan to examine the use of [^{123}I]IMT in diagnosis of disease.

Key words: amino acid transport, artificial amino acid, renal cortex, 3-iodo-α-methyl-L-tyrosine

INTRODUCTION

THE ARTIFICIAL amino acid 3-iodo-α-methyl-L-tyrosine (IMT) has been developed as a functional imaging agent for amino acid transport in the brain and pancreas.[1–3] It has also been successfully used clinically for SPECT imaging of brain tumors and whole-body scintigraphy for tumor imaging.[4–7] Renal physiological accumulation of radiolabeled IMT is higher than that of radiolabeled Tyr. We have also observed marked renal accumulation and rapid urinary excretion of IMT in mice.[8] Clarification of these accumulation mechanisms could aid in development of methods for reducing physiological accumulation, which obstructs abdominal tumor imaging. Also, we

Received January 1, 2004, revision accepted February 19 2004.

For reprint contact: Naoto Shikano, M.S., Department of Radiological Sciences, Ibaraki Prefectural University of Health Sciences, 4669–2 Ami, Ami-machi, Inashiki-gun, Ibaraki 300–0394, JAPAN.

E-mail: sikano@ipu.ac.jp

believe that it would facilitate evaluation of radiolabeled IMT as a renal imaging agent. To investigate the pathways responsible for IMT accumulation in the kidney, we performed IMT uptake and inhibition experiments using ^{125}I-labeled IMT ([^{125}I]IMT) and normal human renal proximal tubule epithelial cells (RPTEC), which are characteristic of the proximal convoluted tubule. Partition coefficients were determined for hypothetic urine at pH ranging from 5 to 8 (hypothetic urine pH). In the *in vivo* experiments using mice, we performed whole body autoradiography and examined biodistribution and excretion inhibition. Also, renal SPECT in a normal canine was performed using ^{123}I-labeled IMT ([^{123}I]IMT).

MATERIALS AND METHODS

Animal experiments were approved by the ethics committees of the affiliated universities.

Materials and preparation of labeled compounds

Reagent-grade 2-amino-bicyclo[2,2,1]heptane-2-carboxylic acid (BCH), 2-(methylamino)isobutyric acid (MeAIB), 2-aminoisobutyric acid (AIB), probenecid, furosemide, ethacrynic acid and α-methyl-L-tyrosine were acquired from Sigma-Aldrich Japan K.K. (Tokyo, Japan). Chloramine-T and other chemicals of reagent grade were purchased from Kanto Chemical Co. (Tokyo, Japan).

The radioisotope [^{125}I]NaI (8.1×10^{19} Bq/mol) was obtained from Amersham Pharmacia Biotech UK (Buckinghamshire, UK). [^{123}I]NaI (8.79×10^{18} Bq/mol) solution was provided by Nihon Medi-Physics Co., Hyogo, Japan. For preparation of labeled compounds, non-carrier-added [^{125}I]IMT, [^{123}I]IMT and 4-[^{125}I]iodo-L-*meta*-tyrosine (4-[^{125}I]*m*Tyr) were prepared by the conventional chloramine-T method, using α-methyl-L-tyrosine as a precursor, as previously reported.[1-3,8] A Nova-Pak C18 (3.9 × 300 mm; Waters, Milford, MA, USA) was used for separation and purification. Silica gel thin-layer chromatography kit (TLC, catalogue number Art. 5553) was obtained from Merck (Darmstadt, Germany). [^{123}I]*N*-isopropyl-*p*-iodoamphetamine ([^{123}I]IMP), technetium-99m-diethylenetriaminepentaacetic acid ([^{99m}Tc]DTPA) and technetium-99m-mercaptoacetylglycylglycylglycine ([^{99m}Tc]MAG3) were acquired from Nihon Medi-Physics Co., Hyogo, Japan.

For cell experiments, normal human renal proximal tubule epithelial cells (RPTEC), which are characteristic of the proximal convoluted tubule, were obtained from Cambrex Bio Science Walkersville, Inc. (Walkersville, MD, USA). Plastic tissue culture flasks (surface area, 25 cm^2) were purchased from Nalge Nunc International (Roskilde, Denmark).

For ^{125}I-labeled compounds, radioactivity was measured using an ARC-380 well-type scintillation counter (Aloka). For ^{14}C-labeled compounds, radioactivity was measured using an LS6500 liquid scintillation counter (Beckman Instruments, Fullerton, CA, USA).

Measurements of partition coefficients

The partition coefficients of [^{125}I]IMT and [^{123}I]IMP were measured using a pre-mixed combination of 2.0 m*l* of *n*-octanol (organic phase) and 2.0 m*l* of 0.1 M phosphate buffer (aqueous phase). The radioactive sample (10 μ*l*; 0.68 kBq) was added to this combination, followed by mixing twice for 1 min each time at room temperature, using a mechanical mixer. After centrifugation, the radioactivity of 0.2 m*l* aliquots was measured.

Cell line study

RPTEC cells were maintained by serial passages in 25-cm^2 cell culture flasks in 8 m*l* of complete medium using REGM™ Bullet Kit (Cambrex Bio Science Walkersville, Inc., Walkersville, MD, USA), in 500 m*l* of REBM™ culture medium and a REGM™ Single Qouts mixture containing hEGF (10 μg/*l*), insulin (5 μg/*l*), hydrocortisone (0.5 μg/*l*), fetal calf serum (0.5%), epinephrine triiodothyronine (0.5 μg/*l*), transferrin (6.5 μg/*l*) and GA-100 (1 m*l*/*l*) in an atmosphere of 5% CO_2: 95% air at 37°C. Subculturing was performed every 4 days using 0.02% EDTA and 0.05% trypsin. Cells were used within the 3rd passage.

Uptake was measured using RPTEC cell semi-confluent monolayers grown on 60 mm plastic culture dishes (Falcon; Becton Dickinson, Lincoln Park, NJ, USA). The incubation medium comprised 145 mM NaCl, 3 mM KCl, 1 mM $CaCl_2$, 0.5 mM $MgCl_2$, and 5 mM 2-hydroxyethylpiperazine-*N*′-2-ethanesulfonic acid (HEPES), with a final pH of 7.4. In the Na^+-dependence experiment, NaCl was replaced with the same concentration of choline-Cl. After removal of culture medium, each dish was washed once with 5 m*l* of incubation medium for 10 min at 37°C. Cells were then incubated with 2 m*l* of incubation medium containing 18.5 kBq of non-carrier-added [^{125}I]IMT for several different time periods at 37°C.

For the inhibition study, L-Tyr, D-Tyr, BCH (an inhibitor of system L in sodium-independent transport, and an inhibitor of system B^0 in sodium-dependent transport) or MeAIB (an inhibitor of system A) was added at a final concentration of 1.0 mM. Cells were incubated for 5 min at 37°C with 18.5 kBq of non-carrier-added [^{125}I]IMT.

After incubation, media were aspirated, and monolayers were rinsed twice rapidly using 5 m*l* of ice-cold incubation medium. Cells were solubilized in 1.5 m*l* of 1 N NaOH. Then, radioactivity associated with solubilized cells was measured.

Measurements of protein binding

Serum protein binding of [^{125}I]IMT, 4-[^{125}I]*m*Tyr, [^{99m}Tc]MAG3 and [^{99m}Tc]DTPA was evaluated by ultrafiltration (Ultracent-10; Tosoh, Tokyo, Japan). A mixture (0.9 m*l*) of [^{125}I]IMT (220 kBq) in saline (20 μ*l*)

and rat serum from a male SD rat (age, 6 weeks) was centrifuged at 3,000 rpm for 10 min at room temperature (Himac CF 7D; Hitachi, Tokyo, Japan). Radioactivity (counts/20 μl) of the initials and filtrates was measured using a well-type scintillation counter (ARC-380; Aloka, Tokyo, Japan); these data were used to determine protein binding and free fraction rates.

Renal accumulation and excretion experiments in mice

Biodistribution and urinary excretion experiments in mice were based on a method described previously.[1,9] For the biodistribution experiment, groups of 5 male ddY mice (weight, 30 g; age, 6 weeks) received 0.1 m*l* of [^{125}I]IMT (18.5 kBq) by injection into the tail vein. Mice were anesthetized with ether inspiration and sacrificed by heart puncture at 1, 3, 5, 10, 15, 30, 60 and 120 min after [^{125}I]IMT administration. Organs were dissected.

For the urinary excretion experiment, groups of 5 ddY male mice (weight, 30 g; age, 6 weeks) were injected with 0.1 m*l* saline containing [^{125}I]IMT (55.5 kBq) via the tail vein, and then placed in metabolic cages under feeding conditions. Urine and feces were collected at 5, 10, 15, 30, 60, 180 and 360 min after [^{125}I]IMT administration.

To examine inhibition of urinary excretion of [^{125}I]IMT, the mice received an injection of probenecid, furosemide or ethacrynic acid (50, 10 and 10 mg/kg bodyweight respectively) with [^{125}I]IMT (55.5 kBq).[10] For probenecid loading, the probenecid was pre-administered via the tail vein 10 min prior to injection of [^{125}I]IMT.[11] Urine was collected 10 min after administration. Radioactivity of samples was quantified using the above-mentioned well-type scintillation counter.

In vivo *whole body autoradiography in mice*

For autoradiography, 0.1 m*l* of [^{125}I]IMT (670 kBq) was injected into the tail vein of male ddY mice (n = 4; weight, 30 g; age, 6 weeks). After 5 min, the mice were sacrificed by inspiration of excess ether, placed in carboxymethyl cellulose embedding medium (Nacalai, Kyoto, Japan), and frozen at −15°C for at least 12 hr. An Autocryotome NA-200F (Nakagawa, Tokyo, Japan) was used to cut 20-μm coronal sections from posterior to anterior. Sections were then dried at −15°C for another 24 hr. Tissue slices were kept in contact with BAS-TR2040 imaging plates (Fuji Photo Film, Kanagawa, Japan) for 24 hr. Images were processed using a BAS 2000 Bio-Imaging Analyzer (Fuji Photo Film).

SPECT imaging of canine abdomen

Canine SPECT was performed as described by Kawai et al.[3] A male beagle dog (body weight, 10 kg) was anesthetized with pentobarbital (Nembutal; Abbott Laboratories, Abbott Park, IL) and positioned on the cradle in supine position. [^{123}I]IMT solution (48 MBq in saline) was injected through the femoral vein. Imaging was performed at 2.5-minute intervals for 60 minutes. The abdominal imaging was performed using a ring-type SPECT-camera (SET-030W; Shimadzu, Kyoto, Japan; FWHM, 12 mm; slice thickness, 24 mm; slice interval, 30 mm).

RESULTS

Materials and preparation of labeled compounds

Labeling of α-methyl-L-tyrosine produced [^{125}I]IMT and [^{123}I]IMT with labeling efficiency of more than 80%. After purification with HPLC, we obtained [^{125}I]IMT and [^{123}I]IMT with greater than 95% radiochemical purity.

Measurements of partition coefficients

Partition coefficients of [^{125}I]IMT and [^{123}I]IMP are shown in Figure 1. At pH 7.0 and 7.4, the partition coefficient of [^{125}I]IMT (−0.714 ± 0.007 and −0.741 ± 0.010,

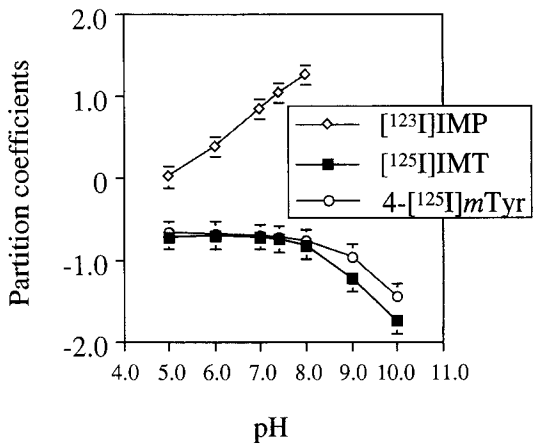

Fig. 1 Partition coefficients of [^{125}I]IMT and [^{123}I]IMP at various pH: log(*n*-octanol/0.1 M phosphate buffer). Values represent the mean ± S.D. (n = 5).

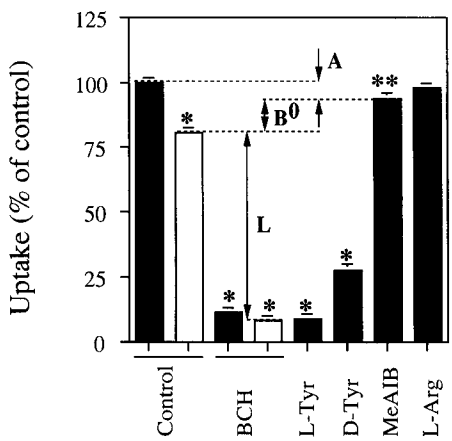

Fig. 2 Effects of inhibitors (1 mM) on accumulation of [^{125}I]IMT in Na^+-containing medium (*black column*) and Na^+-free medium (*white column*). Each column represents mean ± S.D. of 7 to 8 normal human renal proximal tubule epithelial cell monolayers. * $p < 0.001$, ** $p < 0.01$.

respectively) was less than that of [^{123}I]IMP (0.832 ± 0.007 and 1.043 ± 0.009, respectively), which is a well known lipophilic amine.[12] From pH 5 to 8, partition coefficients of [^{125}I]IMT and 4-[^{125}I]*m*Tyr were similarly low.

Cell line study

Time course analysis of [^{125}I]IMT uptake into RPTEC shows that steady-state levels were reached 25 min after starting incubation (data not shown). An incubation time of 10 min was chosen for the inhibition study. The results of the [^{125}I]IMT uptake inhibition experiments are shown in Figure 2. L-Tyr significantly inhibited [^{125}I]IMT uptake ($p < 0.01$). D-Tyr had a smaller inhibitory effect on [^{125}I]IMT uptake than L-Tyr. Replacing sodium with choline significantly reduced [^{125}I]IMT transport into RPTEC cell monolayers.

Transport of [^{125}I]IMT into semi-confluent RPTEC monolayers was predominantly (72.16%) mediated by a Na^+-independent system, with a minor contribution (19.56%) by a Na^+-dependent system (Fig. 2). At 1 mM, the amino acids BCH (with and without sodium) and L-Tyr inhibited accumulation of [^{125}I]IMT at similar magnitudes ($p < 0.001$). This suggests that system B^0 is a main contributor in Na^+-dependent [^{125}I]IMT transport. MeAIB also exhibited a significant inhibitory effect ($p < 0.01$). L-Arg, a basic amino acid, did not inhibit [^{125}I]IMT transport or accumulation (Fig. 2).

Table 1 Protein binding rate in rat serum

Tracer	Protein binding rate (%)	n
[^{125}I]IMT	45.4 ± 5.6	6
4-[^{125}I]*m*Tyr	43.0 ± 8.5	5
[^{99m}Tc]MAG3	80.8 ± 6.3	4
[^{99m}Tc]DTPA	2.3 ± 11.4	5

Values represent mean ± S.D.

Measurements of protein binding

In the *in vitro* binding assay with the SD rat, plasma protein binding of [^{125}I]IMT was approximately 45.4 ± 5.6% (Table 1). The values of other compounds tested are shown in Table 1.

Renal accumulation and excretion experiments in mice

Figure 3 (A) shows kidney accumulation of [^{125}I]IMT (% injected dose/organ) in mice. Peak radioactivity (33.48 ± 6.95%) was observed at 5 min after injection. Kidney-to-other-tissue ratios of [^{125}I]IMT accumulation in mice are shown in Table 2. At 5 min after injection, [^{125}I]IMT accumulation in the kidney was followed by accumulation in the pancreas and adrenal gland, and radioactivity of the kidney was at least 15-fold greater than that of other tissues, except the pancreas and adrenal gland. During the first 30 min, we observed rapid blood clearance (Fig. 3 (A)) and urinary excretion (Fig. 3 (B)) of [^{125}I]IMT. Three hours after administration, more than 70% of the [^{125}I]IMT was found in the urine. At 6 hr after injection, [^{125}I]IMT excretion into feces was only 0.25 ± 0.14%. Figure 4 shows inhibition of urinary excretion of [^{125}I]IMT by drugs in mice. Probenecid, furosemide and ethacrynic acid inhibited urinary excretion of [^{125}I]IMT by 11.10% ($p < 0.01$), 47.21% ($p < 0.01$) and 62.24% ($p < 0.1$),

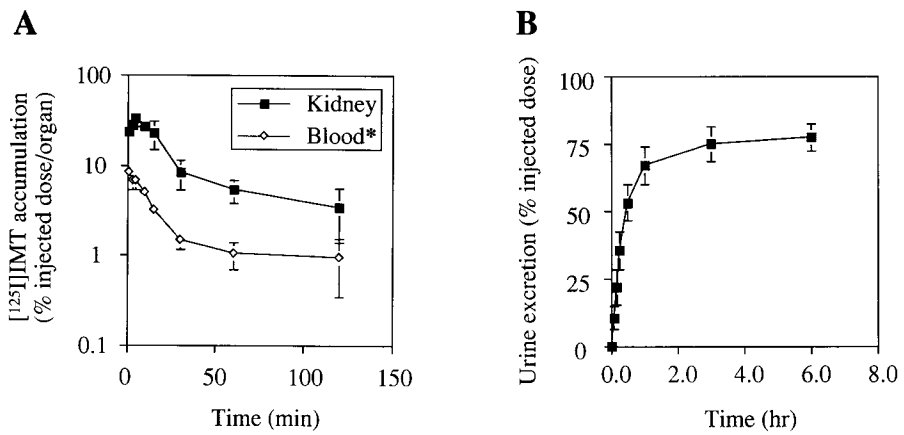

Fig. 3 Kidney accumulation, blood clearance (A) and urinary excretion (B) of [^{125}I]IMT in mice. Values represent the mean ± S.D. (n = 5). *, % injected dose/m*l*.

Table 2 Kidney-to-other-tissue ratios of [^{125}I]IMT accumulation in mice at 5 min after i.v.

Kidney/Blood	Kidney/Pancreas	Kidney/Liver	Kidney/Adrenal	Kidney/Stomach	Kidney/Intestine
15.30 ± 0.53	2.74 ± 0.04	22.17 ± 0.69	4.36 ± 0.01	23.82 ± 0.39	20.20 ± 0.81

Ratio of accumulation: % injected dose/g tissue. Values represent the mean ± S.D. (n = 5).

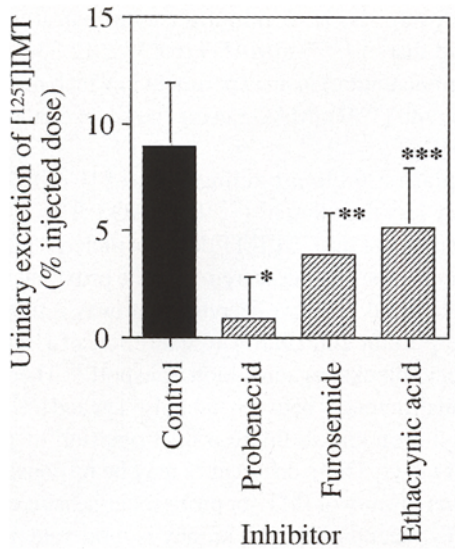

Fig. 4 Inhibition of urinary excretion of [^{125}I]IMT by drugs in mice at 10 min after i.v. Values represent the mean ± S.D. (n = 5). Statistical comparisons between groups were performed using Student's t test. *, $p < 0.01$, **, $p < 0.05$, ***, $p < 0.1$.

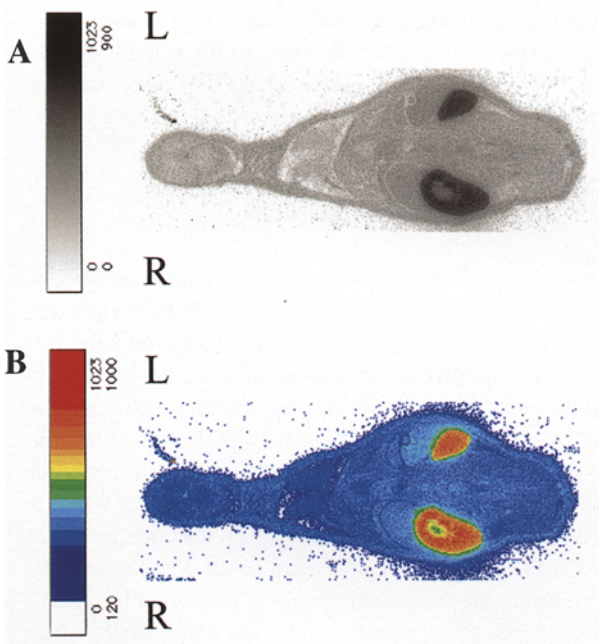

Fig. 5 Whole body autoradiography of [^{125}I]IMT-injected mice at 5 min after i.v., in gray scale (A) and color scale (B).

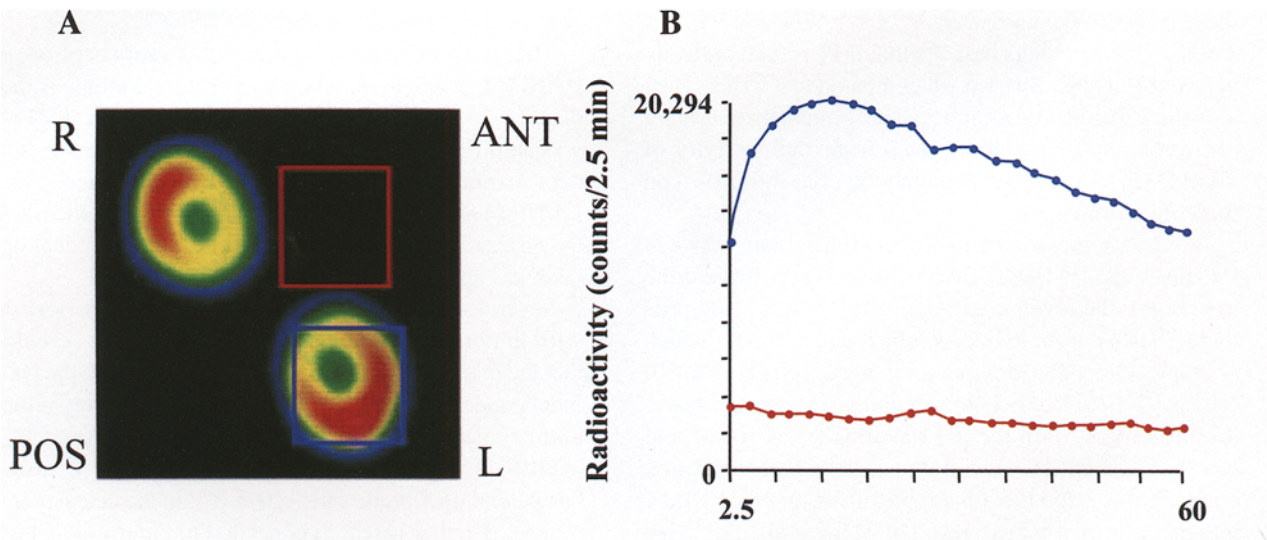

Fig. 6 Preliminary SPECT image of canine abdomen (A) and time-activity curve (B) after intravenous injection of IMT. High accumulation of [^{123}I]IMT in kidney cortex is shown in (A). In (B), red line shows radioactivity of non-target tissue (in the square between the kidneys in (A)), and blue line shows kidney radioactivity (in the square of the left-kidney in (A)). The retention of [^{123}I]IMT in kidney is clearly indicated by the very high ratios of radioactivity in the kidney to background radioactivity in canine abdomen.

respectively, compared to control (100%), at 10 min after administration of [^{125}I]IMT.

In vivo *whole body autoradiography in mice*

Figure 5 shows a typical whole body autoradiograph, demonstrating localization of [^{125}I]IMT in mice at 5 min after administration. The highest radioactivity was found in the kidney. In the kidney, 96.33±1.38% of the [^{125}I]IMT accumulated in the renal cortex, and 3.67 ± 1.38% accumulated in the medulla.

SPECT imaging of canine abdomen

As shown in Figure 6 (A), a clear canine kidney cortex image was obtained. Figure 5 (B) shows that kidney

accumulation peaked at approximately 15 min after injection, followed by gradual decline. At 60 min after injection, retention in kidney was about 65% of peak accumulation. The maximum ratio of kidney count to background count in canine abdomen was approximately 7.0.

DISCUSSION

Metabolically stable IMT has been derived from 3-iodo-L-tyrosine, based on reports that α-methylation confers metabolic stability on L-Tyr,[13,14] and based on a prediction that α-methylation would also confer metabolic stability on 3-iodo-L-tyrosine. We recently examined the fate of injected [^{125}I]IMT and 3-[^{125}I]iodo-L-tyrosine ([^{125}I]IT) in mouse kidney and urine.[1] At 10 min after intravenous injection of [^{125}I]IMT into mice, 94.93 ± 1.43% of radioactivity in the kidney was due to intact [^{125}I]IMT, and 2.21 ± 1.45% was due to deiodinated free I^-; in urine, these respective values were 93.09 ± 2.45% and 3.81 ± 2.00%. Protein incorporation of [^{125}I]IMT was not detected in kidney or any other organs examined. At 10 min after injection of [^{125}I]IT, 14.07 ± 4.55% of radioactivity in the kidney was due to intact [^{125}I]IT, and 75.07 ± 6.13% was due to deiodinated free I^-; in urine, these respective values were 4.79 ± 1.52% and 94.21 ± 1.19%. These findings indicate that IMT is metabolically very stable in the urinary tract, compared to [^{125}I]IT. They also show that neutral amino acid movement up to urinary excretion can be traced by measuring radioactivity of intact IMT; radioactivity of metabolites has little effect on these measurements.

In our comparison of partition coefficients between [^{125}I]IMT and [^{123}I]IMP, from pH 5 to 8 (hypothetic urine pH range), the lower coefficient for [^{125}I]IMT suggests that [^{125}I]IMT is more hydrophilic than [^{123}I]IMP, which is a typical lipophilic compound.[13] Very high pH (8 to 10) causes [^{125}I]IMT to become an anion, increasing its hydrophilicity. Within the pH range of urine, tissue and blood, the [^{125}I]IMT *n*-octanol/phosphate buffer partition coefficient was too low for simple diffusion of [^{125}I]IMT into the cells to occur as a result of its lipophilicity.[13] This indicates that carrier-mediated transport is the main gateway for IMT into the proximal tubule cells under normal blood and urine pH conditions.

We obtained very clear autoradiographs of mouse renal cortex and a canine renal SPECT image (S2-like region). Although we cannot simply compare accumulation levels of IMT and [^{99m}Tc]MAG3 (a clinical renal function imaging radiopharmaceutical), because they are transported by different mechanisms, there are similarities between excretion of IMT and excretion of [^{99m}Tc]MAG3.[11] In both cases, most of the injected compound is excreted into urine with markedly high accumulation in kidney cortex (S2-like region), and excretion into feces is negligible. A surprising finding is that the peak kidney accumulation of [^{125}I]IMT (102.62 ± 0.93% injected dose/g tissue; 5 min after administration)[8] far exceeded that of [^{99m}Tc]MAG3 (64.32 ± 12.83%; 2 min after administration) in an experiment in which mice were injected with [^{99m}Tc]MAG3 using the same method used for [^{125}I]IMT.

The plasma protein binding ratio of [^{125}I]IMT was markedly less than that of [^{99m}Tc]MAG3. This suggests that about half of the [^{125}I]IMT does not undergo glomerular filtration, resulting in secretion in the proximal tubule.

A probenecid-sensitive secretion pathway is thought to be an important contributor to excretion of [^{125}I]IMT. Probenecid blocks organic anion transport.[10] There are 2 structural differences between natural L-Tyr and [^{125}I]IMT: α-methylation and iodination of 3 position of phenol group of L-Tyr. These differences may be responsible for the greater affinity of IMT for probenecid-sensitive secretion. L-Tyr accumulation in kidney is moderate, in contrast to the high accumulation of IMT.[15] Affinity for accumulative organic anion transport system may contribute to the high accumulation of IMT in kidney cortex (proximal tubule of S2-like region). Like probenecid, the diuretics furosemide and ethacrynic acid inhibited secretion of [^{125}I]IMT. It is interesting that these drugs inhibit transport of *p*-aminohippurate (PAH) and [^{99m}Tc]MAG3 via organic anion transporter 1.[11,16,17]

The present results suggest that reabsorption of [^{125}I]IMT in apical membrane of proximal tubule is mediated by system B^0, because [^{125}I]IMT uptake into RPTEC was significantly inhibited by BCH in a sodium-dependent manner. Up to 63.73% of total sodium-dependent [^{125}I]IMT uptake into RPTEC was apparently mediated by system B^0, and the remaining sodium-dependent uptake was apparently mediated by system A.

Several studies on IMT transport have been performed with tumor cell lines.[18–21] These studies have revealed that the majority of IMT transport takes place via the Na^+-independent system L (>70%), and that relatively minor uptake takes place via the Na^+-dependent system $B^{0,+}$ (<20%). Proximal tubule cells have system L in the basolateral membrane and system $B^{0,+}$ in the apical membrane.[22] Further research is needed to determine which isoforms of the transporters in these systems mediate IMT transport in the kidney.

System L is important because some essential amino acids are transported via this system in plasma membrane.[22] Of the system L transporters, human L-type amino acid transporter 1 (hLAT1) and its isoform hLAT2 are the main neutral amino acid transporters in plasma membrane.[23,24] Formation of a hetero-dimer with heavy chain of 4F2 antigen (4F2hc) is required for functional expression of hLAT1 and hLAT2.[23,24] Recently, we examined the isoform selectivity of [^{125}I]IMT transport via hLAT1 and hLAT2 in *Xenopus laevis* oocytes coexpressing 4F2hc.[25] The results indicate that [^{125}I]IMT transport selectively occurs via hLAT1-4F2hc heterodimer, whereas transport of L-Tyr (structural parent of

IMT) was not isoform-selective.[25] Expression of hLAT1 is ubiquitous, and IMT is a substrate of hLAT1.[24–26] In the proximal tubule, hLAT2-4F2hc expression is observed in basolateral membrane of epithelial cells.[23] This isoform is involved in secretion and reabsorption of neutral amino acids, as an amino acid exchanger.[23] Natural amino acids, including mother L-Tyr, are reabsorbed so extensively that only small amounts of natural amino acids are found in urine.[22] Our finding of rapid urinary excretion of [^{125}I]IMT may be due to its lack of affinity for hLAT2-4F2hc.

Radioiodinated amino acids have been used as imaging agents in the majority of tumor imaging studies. Based on the clear image obtained in the present study, we believe that [^{123}I]IMT is a useful imaging agent for kidney studies. Renal amino acid transport is disturbed in a number of diseases. In future studies, we plan to investigate use of IMT in the diagnosis of kidney diseases.

CONCLUSIONS

With high kidney-to-other-tissue ratios, we observed markedly high accumulation of metabolically stable IMT in an S2-like region of kidney cortex in mice. A clear kidney cortex image was obtained in the canine SPECT experiment. Accumulation of IMT is mediated by probenecid-sensitive membrane transport and BCH-sensitive membrane transport in a Na^+-dependent manner. We believe that [^{123}I]IMT is useful for kidney imaging, and we plan to investigate use of IMT in the diagnosis of disease in future studies.

ACKNOWLEDGMENTS

We wish to thank Sae Fujimoto, Yuki Nobayashi, Junko Yagi, and Takashi Kotani (Ibaraki Prefectural University) for their excellent technical assistance. This work was supported by Grants-in-Aid for Scientific Research (#10770451, #14770498, #13557075 and #15659283) from the Ministry of Education, Science, Sports and Culture of Japan and the Japan Society for the Promotion of Science. Financial support was also provided by the Ibaraki Prefectural University Research Project (9808-3, 0118-1 and 0220-1) and an Ibaraki Prefectural University Grants-in-Aid for the Encouragement for Young Scientists 2001, 2002 and 2004.

REFERENCES

1. Kawai K, Fujibayashi Y, Saji H, Yonekura Y, Konishi J, Kubodera A, et al. A strategy for study of cerebral amino acid transport using iodine-123-labeled amino acid radiopharmaceutical: 3-iodo-alpha-methyl-L-tyrosine. *J Nucl Med* 1991; 32: 819–824.
2. Kawai K, Fujibayashi Y, Yonekura Y, Konishi J, Saji H, Kubodera A, et al. An artificial amino acid radiopharmaceutical for single photon emission computed tomographic study of pancreatic amino acid transports ^{123}I-3-iodo-alpha-methyl-L-tyrosine. *Ann Nucl Med* 1992; 6: 169–175.
3. Kawai K, Fujibayashi Y, Yonekura Y, Tanaka K, Saji H, Konishi J, et al. Canine SPECT studies for cerebral amino acid transport by means of ^{123}I-3-iodo-α-methyl-L-tyrosine and preliminary kinetic analysis. *Ann Nucl Med* 1995; 9: 47–50.
4. Biersack HJ, Coenen HH, Stoecklin G, Reichmann K, Bockische A, et al. Imaging of brain tumors with L-3-[I-123]iodo-α-methyl tyrosine and SPECT. *J Nucl Med* 1989; 30: 110–112.
5. Kuwert T, Woesler B, Morgenroth C, Lerch H, Schafers M, Palkovic S, et al. Diagnosis of recurrent glioma with SPECT and iodine-123-α-methyl tyrosine. *J Nucl Med* 1998; 39: 23–27.
6. Jager PL, Franssen EJF, Kool W, Szabo BG, Hoeckstra HJ, Groen HJM, et al. Feasibility of tumor imaging using L-3-[iodine-123]-iodo-alpha-methyl-tyrosine in extracranial tumors. *J Nucl Med* 1998; 39: 1736–1743.
7. Langen K-J, Pauleit D, Coenen HH. 3-[^{123}I]Iodo-α-methyl-L-tyrosine: uptake mechanisms and clinical applications. *Nucl Med Biol* 2002; 29: 625–631.
8. Shikano N, Kawai K, Flores II LG, Nishii R, Kubota N, Ishikawa N, et al. An artificial amino acid 4-iodo-L-*meta*-tyrosine: Biodistribution and excretion via kidney. *J Nucl Med* 2003; 44: 625–631.
9. Flores II LG, Kawai K, Nakagawa M, Shikano N, Jinnouchi S, Tamura S, et al. A new radiopharmaceutical for the cerebral dopaminergic presynaptic function: 6-radioiodinated L-*meta*-tyrosine. *J Cereb Blood Flow Metab* 2000; 20: 207–212.
10. Brazeau P. Inhibitors of tubular transport of organic compounds. In: *The Pharmacologic Basis of Therapeutics*, Goodman L, Gilman A (eds), New York; MacMillan Publishing Co., Inc., 1975: 862–863.
11. Fritzberg AR, Kasina S, Eshima D, Johnson DL. Synthesis and biological evaluation of technetium-99m MAG3 as a hippuran replacement. *J Nucl Med* 1986; 27: 111–116.
12. Winchell SH, Baldwin RM, Lin TH. Development of I-123-labeled amines for brain studies: localization of I-123-iodophenylalkyl amines in rat brain. *J Nucl Med* 1980; 21: 940–946.
13. Cooper JR, Bloom FE, Roth RH. Catecholamine. I. General aspects. In: *The biochemical basis of neuropharmacology*, 5th ed, New York; Oxford University Press, 1984: 203–258.
14. Mimnaugh MN, Gearien JE. Adrenergic drugs. In: *Principles of medicinal chemistry*, 3rd ed, Foye WO (eds), Philadelphia; Lea & Febiger, 1989: 343–358.
15. Jager PL, Vaalburg W, Pruim J, Vries E GE, Langen K-J, Piers DA. Radiolabeled amino acids: Basic aspects and clinical applications in oncology. *J Nucl Med* 2001; 42: 432–445.
16. Sekine T, Watanabe N, Hosoyamada M, Kanai Y, Endou H. Expression cloning and characterization of a novel multispecific organic anion transporter. *J Biol Chem* 1997; 272: 18526–18529.
17. Shikano N, Kanai Y, Kawai K, Ishikawa N, Endou H. Transport of technetium-99m-MAG3 via rat renal organic anion transporter 1. *J Nucl Med* 2004; 45: 80–85.
18. Reimann B, Stoegbauer F, Kopka K, Halffer H, Lasic M, Schirmachr A, et al. Kinetics of 3-[^{123}I]iodo-L-α-methyl tyrosine transport in rat C6 glioma cells. *Eur J Nucl Med*

1999; 26: 1274–1278.
19. Riemann B, Kopka K, Stogbauer F, Halfter H, Ketterler S, Vu Phan TQ, et al. Kinetic parameters of 3-[^{123}I]iodo-L-α-methyl tyrosine ([^{123}I]IMT) transport in human GOS3 glioma cells. *Nucl Med Biol* 2001; 28: 293–297.
20. Franzius C, Kopka K, Valen F, Eckervogt V, Riemann B, Sciuk J, et al. Characterization of 3-[^{123}I]iodo-L-α-methyl tyrosine ([^{123}I]IMT) transport into human Ewing's sarcoma cells *in vitro*. *Nucl Med Biol* 2001; 28: 123–128.
21. Lahotte T, Caveliers V, Dierickx L, Vekeman M, Everaert H, Mertens J, et al. *In vitro* characterization of the influx of 3-[^{125}I]iodo-L-α-methyl tyrosine and 2-[^{125}I]iodo-L-tyrosine into U266 human myeloma cells: Evidence for System T transport. *Nucl Med Biol* 2001; 28: 129–134.
22. Christensen HN. Role of amino acid transport and counter-transport in nutrition and metabolism. *Physiol Rev* 1990; 70: 43–77.
23. Segawa H, Fukasawa Y, Miyamoto K, Takeda E, Endou H, Kanai Y. Identification and functional characterization of a Na^+-independent neutral amino acid transporter with broad substrate selectivity. *J Biol Chem* 1999; 274: 19745–19751.
24. Kanai Y, Segawa H, Miyamoto K, Uchino H, Takeda E, Endou H. Expression cloning and characterization of a transporter for large neutral amino acids activated by heavy chain of 4F2 antigen (CD98). *J Biol Chem* 1998; 273: 23629–23632.
25. Shikano N, Kanai Y, Kawai K, Inatomi J, Kim DK, Ishikawa N, et al. Isoform selectivity of 3-^{125}I-iodo-α-methyl-L-tyrosine membrane transport in human L-type amino acid transporters. *J Nucl Med* 2003; 44: 244–246.
26. Shikano N, Kanai Y, Kawai K, Ishikawa N, Endou H. Characterization of 3-[^{125}I]iodo-α-methyl-L-tyrosine transport via human L-type amino acid transporter 1. *Nucl Med Biol* 2003; 30: 31–37.